

## THERMAL MATHEMATICAL MODEL OF THE H-SHAPED BLOCK OF A NONHERMETIC INSTRUMENTAL COMPARTMENT OF A GEOSTATIONARY SPACECRAFT

V. A. Burakov,<sup>a</sup> V. V. Elizarov,<sup>a</sup>  
E. N. Korchagin,<sup>b</sup> V. P. Kozhukhov,<sup>b</sup>  
A. S. Tkachenko,<sup>a</sup> and I. V. Shcherbakova<sup>a</sup>

UDC 629.78.048.7.001.24

*A dynamic thermal mathematical model in distributed-lumped parameters, a computational algorithm, and a software of numerical calculations have been developed. The results of these calculations for multidimensional nonstationary temperature fields in operation of the on-board devices and a network of uncontrolled heat pipes in a nontraditional H-shaped block of the service-system module of a nonhermetic instrumental compartment of promising durable geostationary spacecraft under the conditions of orbital operation have been obtained.*

A new generation of promising durable (service life is no shorter than 12 years) geostationary spacecraft has a block-modular structure of a parallelepiped-shaped nonhermetic instrumental compartment assembled of large-size, plane, three-layer honeycomb panels and  $\Pi$ -(payload-module block),  $N$ -(information-logical block), and  $U$ -shaped (power-propulsion block) blocks; this block-modular structure performs simultaneously a force function, a thermal function, and a function of protection against outer-space factors [1]. To ensure the thermal regime of the on-board equipment use is made of a passive thermal-control system (PTCS) based on uncontrolled low-temperature heat pipes and optical coatings in combination with electrical heating.

The H-shaped block of a service-system module (SSM) presented in Fig. 1 is a nontraditional structural element, and it makes it possible to employ, partially or completely, all four sides of the nonhermetic instrumental compartment as radiator panels (instead of the North and South panels, as in all modern spacecraft). In the H-shaped block, the instrument panel, having a bilateral layout of the on-board equipment, is thermally connected with the East and West radiator panels by a network of bundles of four heat pipes, located in parallel planes. Excess heat is removed to outer space predominantly from the radiator panel which is in shadow at a given instant of time.

In the present work, we propose a distributed-lumped-parameter dynamic thermal mathematical model of a nontraditional H-shaped block of an SSM with a PTCS based on the uncontrolled low-temperature heat pipes of a nonhermetic instrumental compartment of geostationary spacecraft in orbital service in the diurnal cycle of illumination by the sun.

Without allowance for the shadings, reradiations, and rereflections from the external adjacent elements of the complex structure of geostationary spacecraft, which call for special thorough analysis, the density of the absorbed heat flux in the diurnal cycle of illumination by the sun for the East and West radiator panels of the H-shaped SSM block is expected by the periodic analytical dependence taking into account the shadow portion of the earth at vernal and autumnal equinoctial points [2]:

$$q_s(t) = \begin{cases} 0, & 0 < t \leq 12 \text{ h}, \\ A_s S_0 \sin \theta \sin \left[ \frac{\pi (24 - t)}{12} \right], & 12 \text{ h} < t \leq t_{e,s}, \\ 0, & t_{e,s} < t \leq 24 \text{ h}. \end{cases} \quad (1)$$

<sup>a</sup>Scientific-Research Institute of Applied Mathematics and Mechanics at Tomsk State University, Tomsk, Russia; <sup>b</sup>Academician M. F. Reshetnev Science and Production Association of Applied Mechanics, Zheleznogorsk, Russia; email: bva@niipmm.tsu.su. Translated from *Inzhenerno-Fizicheskii Zhurnal*, Vol. 76, No. 4, pp. 142–149, July–August, 2003. Original article submitted May 6, 2002; revision submitted November 11, 2002.

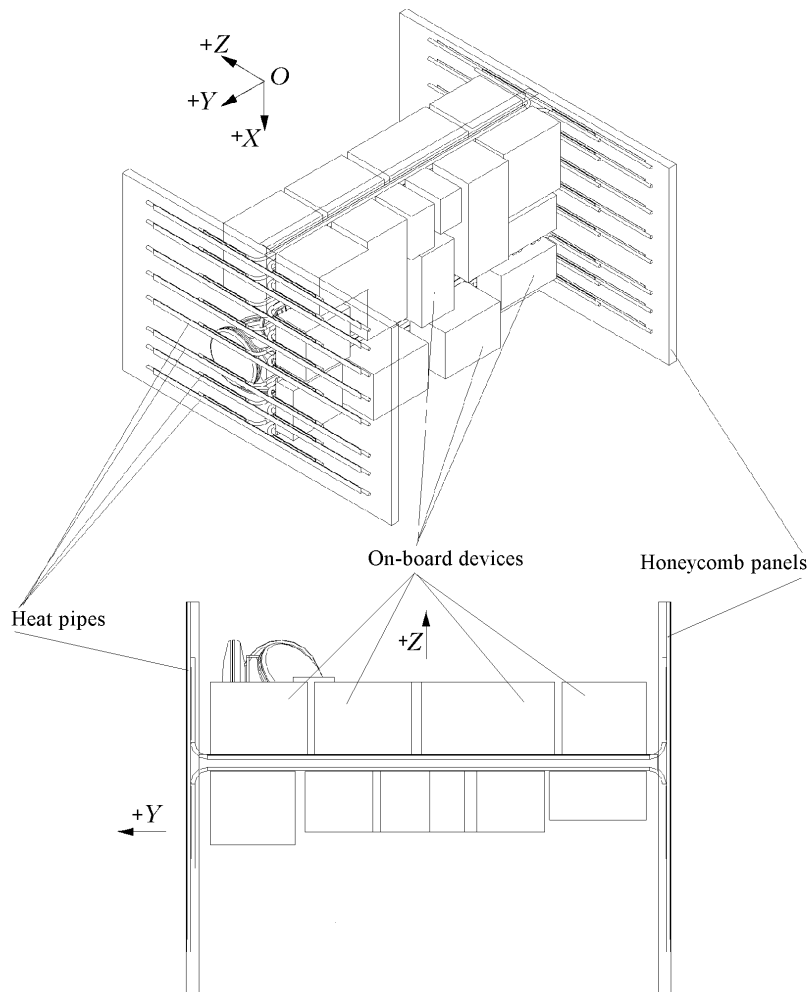


Fig. 1. Structure of the nontraditional H-shaped SSM block of the nonhermetic instrumental compartment of a geostationary spacecraft.  $OXYZ$ , global coordinate system.

The most important parameter in (1) is the capacity of the cooling coating "optical solar reflector" (OSO-S) specially applied to the East and West radiator panels for absorbing direct solar radiation. The quantity  $A_s$  is variable with time and depends on the degree of degradation of OSO-S under the action of outer-space factors, reaching values of 0.33 to 0.4 at the end of a 12–15-year active life for promising durable geostationary spacecraft.

The density of the self-radiation flux from the radiation surfaces of the East and West radiator panels of the H-shaped SSM block is expressed according to the Stefan–Boltzmann law.

The plane rectangular three-layer honeycomb panels of the H-shaped SSM block which are efficient in mass and overall dimensions and ensure the required strength, thermal conductivity, and radiation protection are manufactured in the form of two thin continuous carrier facings of aluminum alloys bonded with a hexagonally structured anisotropic cellular honeycomb filler of aluminum foil of the needed constructional depth and the skeleton elements for strength and mechanical joining in the structure of the nonhermetic instrumental compartment of geostationary spacecraft.

In mathematical modeling of the processes of conductive heat transfer in the three-layer honeycomb panels of the H-shaped SSM block (instrument, East, and West panels), we make the following main assumptions:

1. Calculation of nonstationary temperature fields is carried out for each individual honeycomb panel in the local coordinate system whose  $OZ$  axis is always directed inward.
2. The temperature gradients over the thickness of high-conductive metal facings of the honeycomb panels and skeleton elements are disregarded.

3. The honeycomb filler is considered as a continuous anisotropic (orthotropic) porous medium with effective thermophysical characteristics and a predominant linear propagation of heat along the  $OZ$  axis. Radiation heat exchange is considered to be insignificant for the available temperature differences.

4. The thermophysical characteristics of all the materials used for manufacture of a panel are taken to be constant.

Within the framework of the assumptions made, the distributed-parameter dynamic thermal mathematical model of conductive heat transfer in the three-layer honeycomb panels of the H-shaped SSM block has the following form in the local Cartesian coordinate system  $OXY$ :

$$\frac{\partial T_m}{\partial t} = a_f \left( \frac{\partial^2 T}{\partial x^2} + \frac{\partial^2 T}{\partial y^2} \right) + Q_m, \quad m = 1, 2, \quad 0 < x < L_x, \quad 0 < y < L_y, \quad 0 < t \leq 24 \text{ h}; \quad (2)$$

$$\frac{\partial T_m}{\partial t} = a_{st} \frac{\partial^2 T_m}{\partial \xi^2} + \Phi_m + \Phi_{m\text{cont}}, \quad m = \overline{3, 6}, \quad 0 < \xi < 2(L_x + L_y), \quad 0 < t \leq 24 \text{ h}; \quad (3)$$

$$\left. \frac{\partial T_m}{\partial n} \right|_{\Gamma_m} = 0, \quad m = 1, 2; \quad (4)$$

$$\left. \frac{\partial T_3}{\partial \xi} \right|_{\xi=L_y} = \left. \frac{\partial T_4}{\partial \xi} \right|_{\xi=L_y}, \quad T_3|_{\xi=L_y} = T_4|_{\xi=L_y}; \quad (5)$$

$$\left. \frac{\partial T_4}{\partial \xi} \right|_{\xi=L_y+L_x} = \left. \frac{\partial T_5}{\partial \xi} \right|_{\xi=L_y+L_x}, \quad T_4|_{\xi=L_y+L_x} = T_5|_{\xi=L_y+L_x}; \quad (6)$$

$$\left. \frac{\partial T_5}{\partial \xi} \right|_{\xi=2L_y+L_x} = \left. \frac{\partial T_6}{\partial \xi} \right|_{\xi=2L_y+L_x}, \quad T_5|_{\xi=2L_y+L_x} = T_6|_{\xi=2L_y+L_x}; \quad (7)$$

$$\left. \frac{\partial T_3}{\partial \xi} \right|_{\xi=0} = \left. \frac{\partial T_6}{\partial \xi} \right|_{\xi=2(L_y+L_x)}, \quad T_3|_{\xi=0} = T_6|_{\xi=2(L_y+L_x)}; \quad (8)$$

$$T_m(x, y, 0) = T_{\text{int}}, \quad m = 1, 2, \quad 0 \leq x \leq L_x, \quad 0 \leq y \leq L_y; \quad (9)$$

$$T_m(\xi, 0) = T_{\text{int}}, \quad m = \overline{3, 6}, \quad 0 \leq \xi \leq 2(L_x + L_y). \quad (10)$$

The dynamic thermal mathematical model in distributed parameters (2)–(10) describes the conductive heat transfer in six basic elements of a three-layer honeycomb panel: carrying metal facings (2) and skeleton elements (3) with boundary and initial conditions (4)–(10). The origin of coordinates  $\xi = 0$  coincides with the origin of the Cartesian coordinate system. The skeleton elements are numbered in the direction of the  $OY$  axis. Boundary condition (8) corresponds to periodic problems of nonstationary heat conduction.

The dynamic model (2)–(10) is closed by determination of the source terms  $Q_m$ ,  $\Phi_m$ , and  $\Phi_{m\text{cont}}$  in the non-stationary-heat-conduction equations (2) and (3) responsible for the special properties of the heat exchange in each of the three honeycomb panels of the H-shaped SSM block. For example, for the instrument panel we have

$$Q_1 = \frac{\sum_n q_{s.e1n} - q_{\text{cond1}} - \sum_k q_{h.p1k} - q_{f.st1}}{\delta_{f1} \rho_f c_f}, \quad (11)$$

$$q_{s.e1n} = \frac{P_{s.e1n}}{F_{s.e1n}}, \quad n = \overline{1, N_{s.e1}},$$

$$q_{\text{cond1}} = q_{\text{cond2}} = \frac{\lambda_{\text{eff}}}{\delta_h} \left( \frac{\text{Bi}_{f,h}}{2 + \text{Bi}_{f,h}} \right) (T_1 - T_2),$$

$$q_{h.p1k} = \alpha_{f,pk} [T_1(x, y, t) - T_{v1k}(t)], \quad k = \overline{1, N_{h.p}},$$

$$q_{f.st1} = \alpha_{f.st} [T_1(0, y, t) + T_1(x, L_y, t) + T_1(L_x, y, t) + T_1(x, 0, t) - (T_3 + T_4 + T_5 + T_6)];$$

$$Q_2 = \frac{\sum_n q_{s.e2n} + q_{\text{cond2}} - \sum_k q_{h.p2k} - q_{f.st2}}{\delta_{f2} \rho_f c_f}, \quad (12)$$

$$q_{s.e2n} = \frac{P_{s.e2n}}{F_{s.e2n}}, \quad n = \overline{1, N_{s.e2}},$$

$$q_{h.p2k} = \alpha_{f,pk} [T_1(x, y, t) - T_{v2k}(t)], \quad k = \overline{1, N_{h.p}},$$

$$q_{f.st2} = \alpha_{f.st} [T_2(0, y, t) + T_2(x, L_y, t) + T_2(L_x, y, t) + T_2(x, 0, t) - (T_3 + T_4 + T_5 + T_6)];$$

$$\Phi_3 = \frac{\alpha_{f.st} [T_1(0, y, t) + T_2(0, y, t) - 2T_3]}{h_{st} \rho_{st} c_{st}}; \quad (13)$$

.....

$$\Phi_6 = \frac{\alpha_{f.st} [T_1(x, 0, t) + T_2(x, 0, t) - 2T_6]}{h_{st} \rho_{st} c_{st}}; \quad (14)$$

$$\Phi_{3\text{cont}} = - \frac{\alpha_{\text{cont}} (\bar{T}_3 - \bar{T}_{3\text{cont}})}{\delta_{st} \rho_{st} c_{st}}; \quad (15)$$

$$\Phi_{5\text{cont}} = - \frac{\alpha_{\text{cont}} (\bar{T}_5 - \bar{T}_{5\text{cont}})}{\delta_{st} \rho_{st} c_{st}}; \quad (16)$$

$$\Phi_{4\text{cont}} = \Phi_{6\text{cont}} = 0. \quad (17)$$

Mathematical modeling of the heat and mass transfer in single-shelf uncontrolled low-temperature heat pipes built into the anisotropic honeycomb filler over inner and outer facings of the panels of the H-shaped block of the nonhermetic instrumental compartment is carried out within the framework of conductive (without allowance for the detailed analysis of the hydrodynamics and heat and mass transfer in the vapor channel) dynamic thermal mathematical models in lumped parameters under the following main assumptions:

(1) a bundle of four heat pipes in each of the eight parallel planes operates in the subcritical regime (absence of the hydrodynamic choking, boiling-up, and freezing of the heat-transfer agent);

(2) transfer of heat over the structural elements of a heat pipe in the axial and circumferential directions is insignificant;

(3) vapor is in the state of saturation, and its temperature remains constant along the heat pipe;

(4) the evaporation (condensation) zones of a heat pipe coincide with the longitudinal dimensions of the mounting sites of the on-board devices and with the lengths of the zones of connection of four heat pipes into a bundle;

(5) the coefficients of heat transfer in phase transformations of the heat-transfer agent in the evaporation and condensation zones of a heat pipe are constant.

The dynamic conductive thermal mathematical model in lumped parameters lying in one of the eight parallel planes of a bundle of four heat pipes of the H-shaped SSM block (see Fig. 1) is written in the form of a system of  $14 + N_{s,e1} + N_{s,e2}$  ordinary differential heat-balance equations relative to the average temperatures of the characteristic heat-pipe zones with the corresponding initial conditions:

$$\begin{aligned}\sigma_{f,p1n}(\bar{T}_{11n} - T_{e1n}) &= C_{e1n} \frac{dT_{e1n}}{dt} + \sigma_{e1n}(T_{e1n} - T_{v1}), \\ \sigma_{c13}(T_{v1} - T_{c13}) &= C_{c13} \frac{dT_{c13}}{dt} + \sigma_{p,p13}(T_{c13} - T_{e31}), \\ \sigma_{c14}(T_{v1} - T_{c14}) &= C_{c14} \frac{dT_{c14}}{dt} + \sigma_{p,p14}(T_{c14} - T_{e41}), \\ T_{e1n}(0) &= T_{c13}(0) = T_{c14}(0) = T_{\text{int}}, \quad n = \overline{1, N_{s,e1}};\end{aligned}\tag{18}$$

$$\begin{aligned}\sigma_{f,p2n}(\bar{T}_{12n} - T_{e2n}) &= C_{e2n} \frac{dT_{e2n}}{dt} + \sigma_{e2n}(T_{e2n} - T_{v2}), \\ \sigma_{c23}(T_{v2} - T_{c23}) &= C_{c23} \frac{dT_{c23}}{dt} + \sigma_{p,p23}(T_{c23} - T_{e23}), \\ \sigma_{c24}(T_{v2} - T_{c24}) &= C_{c24} \frac{dT_{c24}}{dt} + \sigma_{p,p24}(T_{c24} - T_{e24}), \\ T_{e2n}(0) &= T_{c23}(0) = T_{c24}(0) = T_{\text{int}}, \quad n = \overline{1, N_{s,e2}};\end{aligned}\tag{19}$$

$$\begin{aligned}\sigma_{p,p13}(T_{c13} - T_{e31}) &= C_{e31} \frac{dT_{e31}}{dt} + \sigma_{e31}(T_{e31} - T_{v3}), \\ \sigma_{p,p23}(T_{c23} - T_{e32}) &= C_{e32} \frac{dT_{e32}}{dt} + \sigma_{e32}(T_{e32} - T_{v3}), \\ \sigma_{c31}(T_{v3} - T_{c31}) &= C_{c31} \frac{dT_{c31}}{dt} + \sigma_{f,p,c31}(T_{c31} - \bar{T}_{2c31}),\end{aligned}$$

$$\sigma_{c32} (T_{v3} - T_{c32}) = C_{c32} \frac{dT_{c32}}{dt} + \sigma_{f,p,c32} (T_{c32} - \bar{T}_{2c32}), \quad (20)$$

$$\sigma_{c33} (T_{v3} - T_{c33}) = C_{c33} \frac{dT_{c33}}{dt} + \sigma_{f,p,c33} (T_{c33} - \bar{T}_{2c33}),$$

$$T_{e31} (0) = T_{e32} (0) = T_{c31} (0) = T_{c32} (0) = T_{c33} (0) = T_{int};$$

$$\sigma_{p,p14} (T_{c14} - T_{e41}) = C_{e41} \frac{dT_{e41}}{dt} + \sigma_{e41} (T_{e41} - T_{v4}),$$

$$\sigma_{p,p24} (T_{c24} - T_{e42}) = C_{e42} \frac{dT_{e42}}{dt} + \sigma_{e42} (T_{e42} - T_{v4}),$$

$$\sigma_{c41} (T_{v4} - T_{c41}) = C_{c41} \frac{dT_{c41}}{dt} + \sigma_{f,p,c41} (T_{c41} - \bar{T}_{2c41}),$$

$$\sigma_{c42} (T_{v4} - T_{c42}) = C_{c42} \frac{dT_{c42}}{dt} + \sigma_{f,p,c42} (T_{c42} - \bar{T}_{2c42}), \quad (21)$$

$$\sigma_{c43} (T_{v4} - T_{c43}) = C_{c43} \frac{dT_{c43}}{dt} + \sigma_{f,p,c43} (T_{c43} - \bar{T}_{2c43}),$$

$$T_{e41} (0) = T_{e42} (0) = T_{c41} (0) = T_{c42} (0) = T_{c43} (0) = T_{int}.$$

The system of equations (18)–(21) is open, since we do not know the average temperatures of the saturated vapor in the bundle of four heat pipes:  $T_{v1}(t)$ ,  $T_{v2}(t)$ ,  $T_{v3}(t)$ , and  $T_{v4}(t)$ . The closure condition is formulated based on the law of conservation of energy in the vapor channel of each heat pipe in the known quasistationary form

$$\sum_n \sigma_{e1n} (T_{e1n} - T_{v1}) + \sigma_{c13} (T_{c13} - T_{v1}) + \sigma_{c14} (T_{c14} - T_{v1}) = 0, \quad n = \overline{1, N_{s,e1}}; \quad (22)$$

$$\sum_n \sigma_{e2n} (T_{e2n} - T_{v2}) + \sigma_{c23} (T_{c23} - T_{v2}) + \sigma_{c24} (T_{c24} - T_{v2}) = 0, \quad n = \overline{1, N_{s,e2}}; \quad (23)$$

$$\sigma_{e31} (T_{e31} - T_{v3}) + \sigma_{e32} (T_{e32} - T_{v3}) + \sum_i \sigma_{c3i} (T_{c3i} - T_{v3}) = 0, \quad i = \overline{1, 3}; \quad (24)$$

$$\sigma_{e41} (T_{e41} - T_{v4}) + \sigma_{e42} (T_{e42} - T_{v4}) + \sum_i \sigma_{c4i} (T_{c4i} - T_{v4}) = 0, \quad i = \overline{1, 3}. \quad (25)$$

According to the classification made in [3], the developed dynamic thermal mathematical model (1)–(25) in the nontraditional H-shaped SSM block (carrying thermally loaded on-board equipment) of the nonhermetic instrumental compartment of a geostationary spacecraft in real physical time for the conditions of orbital operation belongs to second-level thermal models in which the thermal states of the singled-out most important elements of the structure and the PTCS are described in distributed and lumped parameters.

Mathematical modeling (1)–(25) results in coordinate- and time-dependent multidimensional nonstationary temperature fields in the three-layer honeycomb panels (instrument, East, and West) of the H-shaped SSM block and temperatures at the calculation nodes of the PTCS of the network of uncontrolled heat pipes in operation of the devices

of the on-board equipment in the diurnal cycle of illumination by the sun. The temperature fields obtained are subsequently employed for extremum analysis of the thermal regimes of the on-board equipment by the maximum and minimum temperatures under the assumption, just as in [2], that the entire scattered thermal power is supplied to the mounting sites of the devices.

Numerical realization of the nonstationary equations of heat conduction in carrying facings (2) was carried out by the finite-difference method according to the noniterative economical two-layer scheme of splitting (fractional steps) with the Yanenko balance [4] on a fixed irregular grid. Numerical solution of the nonstationary equations of heat conduction in the skeleton elements (3) was carried out along the marching coordinate by the cyclic-fitting method [5], while the systems of ordinary differential equations of first order (18)–(21) used for determination of the running temperatures in the evaporation and condensation zones of heat pipes were numerically solved according to the implicit scheme of second order of accuracy upon reduction to the Cauchy problem. Provision was made for controlling the computations on each time layer by checking the total integral heat balance in the three-layer honeycomb panels of the H-shaped SSM block, local heat balances at the mounting sites of all the heat-generating devices of the on-board equipment, and the integral heat balance in operation of the bundles of four heat pipes.

We have created a procedure of automatic generation of the irregular grid, involving the construction of a geometric grid which singles out all the inhomogeneities (mounting sites of the devices, lines of laying of the heat pipes, and heat-insulated zones) inherent in a given thermal problem and a narrower grid for calculation of nonstationary conductive heat transfer.

We have developed and debugged a version of the ILB1 computer program in the high-level algorithmic language Visual C++(v.6.0) for IBM-compatible personal computers. The typical time of calculation of one variant according to the ILB1 program on nonuniform  $43 \times 48$  (instrument panel) and  $35 \times 39$  (East and West radiator panels) grids with a time step of  $\tau = 20$  sec (conductive heat transfer) and  $\tau = 0.1$  sec (heat and mass transfer in the heat pipe) on a Pentium III personal computer (733 MHz) was about 3 min in the diurnal cycle of illumination by the sun, which is quite acceptable for multiparametric numerical calculations. The accuracy for the integral heat balance on the panels and the local heat balance at the mounting sites of the devices was no worse than 3.7 and 7.4% respectively.

The results of the numerical calculations of the nonstationary multidimensional temperature fields in the three-layer honeycomb panels and the operating parameters of heat pipes in the H-shaped SSM block of the nonhermetic instrument compartment were processed using modern technologies of graphical and multiplication visualization and color computer animation.

According to the ILB1 program created, we calculated numerically (on a Pentium-III personal computer, 733 MHz) multidimensional nonstationary temperature fields in the H-shaped SSM block of a promising durable geostationary spacecraft with a total heat release of the on-board equipment of 453 W (metal facing 1) and 230 W (metal facing 2) of the instrument panel and the PTCS based on bundles of four ammonia uncontrolled low-temperature heat pipes (located in eight parallel lying planes) of single-shelf profile (AS-KRA7.5-R1) from AD-31-T5 aluminum alloy (All-Union State Standard 4784-74) with a cylindrical groove capillary structure; the pipes were developed at the Laboratory of Heat Pipes of the National Technical University "Kiev Polytechnic Institute" of Ukraine [6]. Consideration was given to the conditions of orbital operation in the regime of communication session at the end of a 10–12-year active life ( $A_s = 0.33$  and  $\theta = 66.5^\circ$ ) at the vernal equinoctial point ( $S_0 = 1400 \text{ W/m}^2$ ) in the diurnal cycle of illumination by the sun  $0 < t \leq 22.8$  h and of the shadow portion of the earth  $22.8 < t \leq 24$  h. The time was reckoned from the beginning of illumination of the East radiator panel. We employed the following set of initial data:

linear dimensions of the East and West radiator panels  $1.2 \times 2 \times 0.5$  m;

linear dimensions of the instrument panel  $1.2 \times 1.9 \times 0.07$  m;

$\delta_{f1} = \delta_{f2} = 10^{-3}$  m;

$\rho_f = 2700 \text{ kg/m}^3$ ,  $\lambda_f = 130 \text{ W/(m}\cdot\text{K)}$ , and  $c_f = 880 \text{ J/(m}\cdot\text{K)}$ ;

$\delta_h = 48 \cdot 10^{-3}$  m (East and West radiator panels) and  $\delta_h = 68 \cdot 10^{-3}$  m (instrument panel);

$\lambda_{\text{eff}} = 1.48 \text{ W/(m}\cdot\text{K)}$  (thickness of the foil  $4 \cdot 10^{-5}$  m, size of a honeycomb cell  $5 \cdot 10^{-3}$  m, thermal conductivity of the foil material  $120 \text{ W/(m}\cdot\text{K)}$ );

parameters of the heat pipes: outside diameter  $14 \cdot 10^{-3}$  m, inside diameter  $12 \cdot 10^{-3}$  m, width of the shelf 0.3 m, mass per unit length 0.31 kg/m, and coefficients of heat transfer in phase transformations in the evaporation and condensation zones  $7000 \text{ W/(m}^2\cdot\text{K)}$ ;

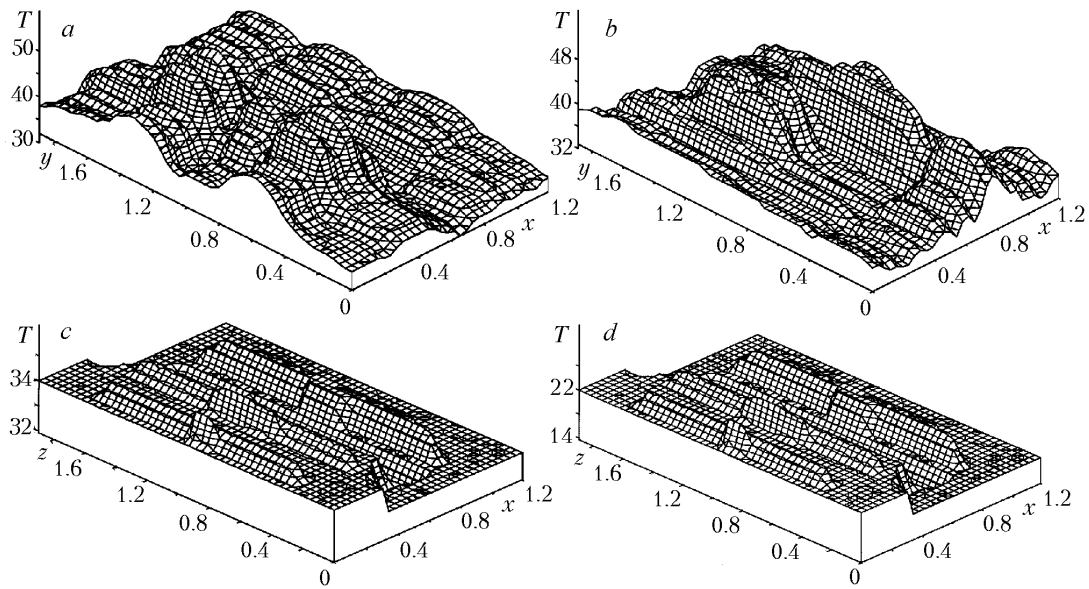


Fig. 2. Spatial distributions of the temperature fields of the metal facing 1 of the instrument panel (a), the metal facing 2 of the instrument panel (b), the metal facing 2 of the East radiator panel (c), and the metal facing 2 of the West radiator panel (d).  $T$ , °C;  $x$ ,  $y$ ,  $z$ , m.

specific thermal resistance of the adhesive joint:

(a) of the heat-pipe shelf and the facing of the panel —  $4 \cdot 10^{-3}$  ( $\text{m}^2 \cdot \text{K})/\text{W}$ ;

(b) of the heat pipes through the shelves —  $10^{-3}$  ( $\text{m}^2 \cdot \text{K})$ ; joint length 0.3 m;

(c) between the facing and the honeycomb filler —  $10^{-3}$  ( $\text{m}^2 \cdot \text{K})/\text{W}$ ;

(d) of the facing and the skeleton element —  $0.14$  ( $\text{m}^2 \cdot \text{K})/\text{W}$ ;

specific thermal resistance of the contact of two honeycomb panels  $0.02$  ( $\text{m}^2 \cdot \text{K})/\text{W}$ ;

integral emissive power of the OSO-S of the East and West radiator panels 0.85;

the zones of radiation surfaces ( $0.22 \times 1.2$  m) are covered with a layer of vacuum-shield heat insulation at the edges of the East and West radiator panels;

$$T_{\text{int}} = 20^\circ\text{C}.$$

Results of the numerical calculations of the multidimensional nonstationary temperature fields of the aluminum-alloy metal facings 1 and 2 of the instrument panel of the H-shaped SSM block in orbital operation at the instant of time  $t = 6$  h are shown in Fig. 2a and b in the global coordinate system (see Fig. 1). As is seen, there is a pronounced orientation of the isotherms along the lines of laying of the heat pipes. The maximum  $q_{s,e}$  corresponded to the maximum temperatures of the mounting sites of the devices; they were  $53.2^\circ\text{C}$  (facing 1) and  $49.6^\circ$  (facing 2). In actual practice, in considering the operation of the H-shaped block as part of the SSM, the level of these temperatures will be lower due to the internal radiation heat exchange. The degree of nonisothermicity of the temperature fields at the mounting sites of the devices attained values of  $16.3$ – $18.6^\circ\text{C}$  (facing 1) and  $10.6$ – $12.2^\circ\text{C}$  (facing 2). The saturated-vapor temperature of the eight heat pipes was within  $30.3$ – $36.7^\circ\text{C}$  (facing 1) and  $33.1$ – $35.8^\circ\text{C}$  (facing 2).

Corresponding results of the numerical calculations of the multidimensional nonstationary temperature fields of the metal facings 2 (radiation surfaces) of the East and West radiator panels are shown in Fig. 2c and d.

The dynamics of change in the daily average temperatures of the metal facings of the three honeycomb panels of the H-shaped SSM block with allowance for the shadow portion of the earth is presented in Fig. 3. Their maximum difference over the instrument-panel thickness was  $1.2^\circ\text{C}$ . The equality of the average temperatures of the metal facings of the East and West radiator panels was attained at the instant of time  $t = 12$  h because of the absence of heating by solar radiation. The maximum temperatures of the mounting sites of the on-board equipment on the metal facings 1 and 2 of the instrument panel were  $10$ – $12^\circ\text{C}$  higher than the maximum average temperatures at the instant of time  $t = 6$  h.



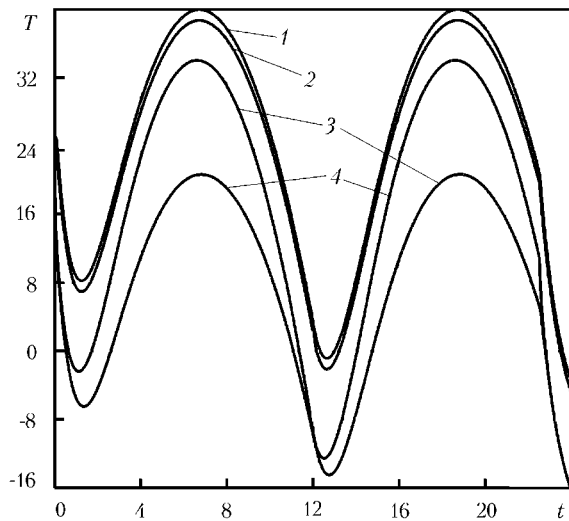


Fig. 3. Dynamics of diurnal change in the average temperatures of the metal facings of the honeycomb panels of the H-shaped SSM block: 1) instrument panel (facing 1); 2) instrument panel (facing 2); 3) East radiator panel (facing 2); 4) West radiator panel (facing 2).  $T$ , °C;  $t$ , h.

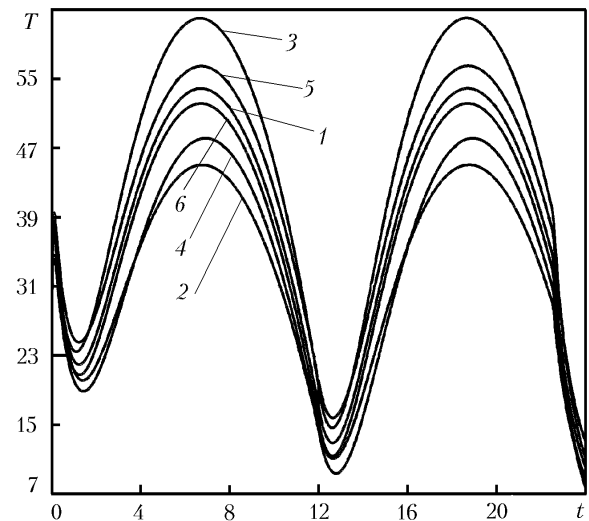


Fig. 4. Dynamics of diurnal change in the maximum temperatures at the mounting sites of the on-board equipment of the metal facing 1 of the instrument panel as a function of different factors: 1) reference calculation; 2)  $A_s = 0.26$ ; 3)  $A_s = 0.4$ ; 4)  $\delta_f = 1.5 \cdot 10^{-3}$  m; 5)  $\alpha_{p,p} = 500$  W/(m<sup>2</sup>·K); 6)  $\epsilon_2 = 0.87$ .  $T$ , °C;  $t$ , h.

The heat exchange of the H-shaped SSM block has a substantially nonstationary character in the diurnal cycle of alternate-periodic action of the external solar flux. However it turned out that the level of maximum temperatures at the mounting sites of the devices of the on-board equipment can be predicted in the stationary regime "overheating" when a constant solar heat flux acts, for example, on the East radiator panel. In this case, the maximum temperatures were equal to 54.5°C (facing 1) and 48.4° (facing 2) and they differed very insignificantly from the results of reference calculation at  $t = 6$  h.

The density of the layout of the on-board equipment on the instrument panel of the H-shaped SSM block is rather high. In this connection, we carried out numerical calculations of the multidimensional nonstationary temperature fields of the metal facings of the instrument panel for the heat-flux densities  $q_{s,e}$  averaged over the entire surface. The maximum temperatures here were 35.4°C (facing 1) and 39.9°C (facing 2) at the instant of time  $t = 6$  h, i.e., they were substantially understated as compared to the results of the reference calculation.

The dynamics of change in the maximum daily temperature of the mounting sites of the on-board equipment of the instrument panel (facing 1) with allowance for the influence of different factors is presented in Fig. 4. At the instant of time  $t = 6$  h, the decrease in the coefficient of absorption of direct solar radiation to  $A_s = 0.26$  (seven-year active life) decreased the maximum temperature by 8.8°C whereas the increase to  $A_s = 0.4$  (15-year active life) cause its inadmissible growth of 8.1°C. The thickening of the metal facings of the instrument panel led to a decrease of 6.2°C in the maximum temperature, while a twofold decrease in the coefficient of contact thermal conductivity between the instrument and radiator heat pipes led to an increase of 2.5°C in it. The change in the coefficient of effective thermal conductivity of the honeycomb filler from 1/48 to 2/96 W/(m·K) exerted no appreciable influence on the value of the maximum temperature. The qualitative character of the influence of the above factors was also preserved for the maximum temperatures of the mounting sites of the on-board equipment of the instrument panel (facing 2).

The use of the PTCS based on of uncontrolled low-temperature heat pipes in a nontraditional H-shaped SSM block has a limitation on the maximum permissible value of  $A_s$ . In the variant of layout of the devices of the on-board equipment and the scheme of laying of the heat pipes in question, the undesirable effect of the transfer of heat from the outer facings (overheated by the sun) of the radiator panels on the weakly heat-releasing on-board equipment of

the instrument panel (facing 2) began to show itself for  $A_s = 0.33$  in one bundle of four heat pipes and for  $A_s = 0.42$  in seven bundles of four heat pipes.

Thus, the developed thermal mathematical model in distributed-lumped parameters enabled us to reveal the fundamental picture and range of diagnostic variables of nonstationary heat exchange of the nontraditional H-shaped SSM block with a PTCS based on a network of uncontrolled low-temperature heat pipes of the nonhermetic instrument compartment of promising durable geostationary spacecraft under the conditions of orbital operation.

## NOTATION

$a$ , thermal-diffusivity coefficient,  $\text{m}^2/\text{sec}$ ;  $A_s$ , integral (total) hemispherical absorptivity;  $\text{Bi}_{f,h} = \frac{\alpha_{f,h}\delta_h}{\lambda_{\text{eff}}}$ , Biot number of contact heat exchange through the adhesive joint between the facing and the honeycomb filler;  $c$  and  $C$ , specific and total heat capacities,  $\text{J}/(\text{kg}\cdot\text{K})$  and  $\text{J}/\text{K}$ ;  $\Gamma$ , boundary;  $F$ , area,  $\text{m}^2$ ;  $h$ , height,  $\text{m}$ ;  $L_x$  and  $L_y$ , linear dimensions of the panel,  $\text{m}$ ;  $n$ , external normal;  $N_{h,p}$  and  $N_{s,e}$ , number of the heat pipes and the on-board devices;  $P$ , heat-release power of the device,  $\text{W}$ ;  $q$ , heat-flux density,  $\text{W}/\text{m}^2$ ;  $Q_m$ , source term in (2),  $\text{K}/\text{sec}$ ;  $S_0$ , density of the flux of direct solar radiation,  $\text{W}/\text{m}^2$ ;  $t$ , time,  $\text{sec}$ ;  $T$ , temperature,  $\text{K}$ ;  $\bar{T}$ , mean-integral temperature,  $\text{K}$ ;  $\Phi_m$  and  $\Phi_{m\text{cont}}$ , source terms in (3),  $\text{K}/\text{sec}$ ;  $x$ ,  $y$ , Cartesian coordinates,  $\text{m}$ ;  $\alpha$ , coefficient of contact thermal conductance,  $\text{W}/(\text{m}^2\cdot\text{K})$ ;  $\delta$ , thickness,  $\text{m}$ ;  $\varepsilon$ , integral (total) hemispherical emissivity;  $\theta$ , angle between the normal to the North and South instrument-radiator panels and the direction to the sun,  $\text{rad}$ ;  $\lambda$ , thermal-conductivity coefficient,  $\text{W}/(\text{m}\cdot\text{K})$ ;  $\rho$ , density,  $\text{kg}/\text{m}^3$ ;  $\xi$ , marching coordinate along the perimeter (skeleton elements) of the honeycomb panel,  $\text{m}$ ;  $\tau$ , time step;  $\sigma$ , thermal conductance,  $\text{W}/\text{K}$ ;  $\sigma_0$ , Stefan–Boltzmann constant,  $\text{W}/(\text{m}^4\cdot\text{K}^4)$ . Subscripts: cont, contact of two honeycomb panels; cond, conductive; c, condensation zone; eff, effective; e.s, earth's shadow portion; e, evaporation zone; f, facing; f.h, contact of the facing with the honeycomb filler; f.st, contact of the facing with the skeleton elements; f.p, contact of the facing with the heat pipe; h, honeycomb filler; h.p, heat pipe; int, initial conditions;  $k$ ,  $m$ , and  $n$ , ordinal numbers; p.p, contact of two heat pipes; s.e, on-board device (on-board-equipment sensor); st, skeleton elements; s, direct solar radiation; v, saturated vapor; 1 and 2, carrying facings in (2)–(17); 3, 4, 5, and 6, elements of the skeleton of the three-layer honeycomb panel in (2)–(17); 1 and 2, heat pipes located in the instrument panel in (18)–(25); 3 and 4, heat pipes located on the East and West radiator panels in (18)–(25).

## REFERENCES

1. Patent 2092398 MKI B6461/10.
2. V. A. Burakov, E. N. Korchagin, V. P. Kozhukhov, et al., *Inzh.-Fiz. Zh.*, **73**, No. 1, 113–124 (2000).
3. B. M. Pankratov, *Thermal Design of Aircraft Units* [in Russian], Moscow (1981).
4. N. N. Yanenko, *Subincremental Method for Solving Multidimensional Problems of Mathematical Physics* [in Russian], Novosibirsk (1967).
5. A. A. Samarskii, *Theory of Difference Schemes* [in Russian], Moscow (1982).
6. B. Rassamakin, G. Tarasov, V. Kozhukhov, et al., in: *Proc. 12th Int. Heat Pipe Conf.*, May 19–24, 2002, Session C1, Moscow–Kostroma–Moscow, Vol. 1 (2002), pp. 62–67.